frontiers in Marine Science

ORIGINAL RESEARCH
published: 28 October 2021
doi: 10.3389/fmars.2021.756076

Tracing the Atmospheric Input of Seawater-Dissolvable Pb Based on the Budget of ^{210}Pb in the East Sea (Japan Sea)

Hojong Seo[1], Guebuem Kim[1], Young-Il Kim[2] and Intae Kim[3]*

[1] School of Earth and Environmental Sciences, Research Institute of Oceanography, Seoul National University, Seoul, South Korea, [2] East Sea Research Institute, Korea Institute of Ocean Science and Technology, Uljin, South Korea, [3] Marine Environmental Research Center, Korea Institute of Ocean Science and Technology, Busan, South Korea

In order to determine the atmospheric input of ^{210}Pb and seawater-dissolvable Pb in the East Sea (Japan Sea), we measured the concentrations of total ^{210}Pb and dissolved Pb (<0.2 μm) in seawater and ^{210}Pb and ^{226}Ra in sinking particles. The East Sea is deep (~3700 m) and enclosed by surrounding continents except for the shallow sills (<150 m). Since the East Sea is located off the East Asian continent under the westerlies, the concentrations of ^{210}Pb and dissolved Pb in this sea are significantly affected by terrestrial sources through the atmosphere. The vertical profiles of total ^{210}Pb and dissolved Pb generally showed a surface maximum and then decreased with depth. The concentrations of dissolved Pb in the surface water were 2 and 3 times higher than those in the North Pacific and North Atlantic Oceans, respectively. Using an independent box model (upper 1000 m or 2000 m), we estimate the atmospheric input of ^{210}Pb to be 1.46 ± 0.25 dpm cm^{-2} y^{-1}, which is within the range of published results from the land-based sites (0.44–4.40 dpm cm^{-2} y^{-1}) in South Korea, China, and Japan. Based on this flux, the residence time of total ^{210}Pb in the East Sea is calculated to be approximately 7.1 ± 1.6 years, which is twice lower than the previous estimation. Combining the residence time of ^{210}Pb and the inventory of dissolved Pb, the atmospheric input of seawater-dissolvable Pb is estimated to be 0.98 ± 0.28 nmol cm^{-2} y^{-1}. This flux is approximately 25% of the Pb flux through the wet deposition (acid-leachable fraction). Thus, our results suggest that the flux and fate of atmospheric Pb in the ocean can be successfully determined using an accurate mass balance model of naturally occurring ^{210}Pb.

Keywords: East Sea, Japan Sea, ^{210}Pb, seawater-dissolvable Pb, atmospheric input

OPEN ACCESS

Edited by:
Selvaraj Kandasamy, Xiamen University, China

Reviewed by:
Edward Boyle, Massachusetts Institute of Technology, United States
Mark Baskaran, Wayne State University, United States

****Correspondence:***
Guebuem Kim
gkim@snu.ac.kr

Specialty section:
This article was submitted to Marine Biogeochemistry, a section of the journal Frontiers in Marine Science

Received: *10 August 2021*
Accepted: *05 October 2021*
Published: *28 October 2021*

Citation:
Seo H, Kim G, Kim Y-I and Kim I (2021) Tracing the Atmospheric Input of Seawater-Dissolvable Pb Based on the Budget of ^{210}Pb in the East Sea (Japan Sea). Front. Mar. Sci. 8:756076. doi: 10.3389/fmars.2021.756076

INTRODUCTION

The naturally occurring radionuclide ^{210}Pb ($t_{1/2}$ = 22.3 years), belonging to the ^{238}U decay series, is produced from ^{226}Ra ($t_{1/2}$ = 1600 years), via ^{222}Rn ($t_{1/2}$ = 3.8 days) and other short-lived radionuclides ($t_{1/2}$ < 30 min). In the upper ocean, most of the ^{210}Pb originates from atmospheric deposition, while that in the deep ocean is mainly produced by *in situ* decay of ^{226}Ra. Therefore, an excess of ^{210}Pb over ^{226}Ra (^{210}Pb$_{ex}$: ^{210}Pb-^{226}Ra) is observed in the upper ocean, except for the polar regions, where the atmospheric input of ^{210}Pb is small (Elsässer et al., 2011; Persson and Holm, 2014; Baskaran and Krupp, 2021). ^{210}Pb is rapidly removed by particles in the surface water,

so the residence time of ^{210}Pb in the surface water is short: 1–3 years in the North Pacific and North Atlantic Oceans (Nozaki and Tsunogai, 1973, 1976; Bacon et al., 1976; Nozaki et al., 1976; Rigaud et al., 2015). The occurrence of $^{210}Pb_{ex}$ decreases toward the continent as enhanced scavenging occurs at the ocean margin (Bacon et al., 1976; Nozaki et al., 1976; Anderson et al., 1994; Seo et al., 2021).

^{210}Pb has been useful in tracing the behavior of anthropogenic Pb in marine environments. For example, the atmospheric input of Pb was estimated using Pb/^{210}Pb ratios in the rain and the steady-state ^{210}Pb flux (Settle et al., 1982). The decreasing trend of anthropogenic Pb flux to the Sargasso Sea in response to decline in the emission of United States leaded gasoline was revealed based on the reduced Pb/^{210}Pb ratios in the surface water from 1979 to 1987 (Boyle et al., 1986; Shen and Boyle, 1988; Sherrell et al., 1992). Those studies also combined the Pb/^{210}Pb ratios with ^{3}H-^{3}He thermocline ventilation model (Jenkins, 1980) to reveal the importance of isopycnal transport on Pb distributions in that region. Sherrell et al. (1992) also suggested that dissolved Pb and particulate Pb were in equilibrium within the residence time of particulate matter based on the Pb isotope ratios (^{206}Pb/^{207}Pb) and ^{210}Pb in suspended particulate matter. However, these ^{210}Pb applications included significant uncertainties since it is difficult to constrain the actual inputs of atmospheric ^{210}Pb to the specific ocean region. In previous studies, the atmospheric input of ^{210}Pb has been estimated by sampling the aerosol and/or rain from the land (islands or coastal sites) (e.g., Turekian et al., 1983; Turekian, 1989), sampling the aerosol and/or rain from the ocean via research cruise (e.g., Rengarajan and Sarin, 2004; Niedermiller and Baskaran, 2019), and modeling (e.g., Turekian et al., 1977; Feichter et al., 1991; Balkanski et al., 1993). However, the land-based sampling methods cannot cover vast areas of the ocean and the sampling during cruise covers only a limited time period. The models also suffer from the lack of measured data (Nozaki et al., 1998), although their results with the measured data can be more representative.

The East Sea (Japan Sea) is an enclosed deep marginal sea in the northwestern Pacific Ocean, with a maximum depth of 3700 m and a surface area of 1.0×10^6 km^2. This sea has a deep water formation and a meridional overturning circulation similar to the global ocean (Ichiye, 1984; Gamo, 1999; Kim et al., 2001), although the turnover time of deep water (∼100 years) is shorter than the global circulation time (Watanabe et al., 1991; Tsunogai et al., 1993; Kumamoto et al., 1998). Since the East Sea does not have a large discharge from rivers and is located off the eastern part of the Asian continent, large amounts of lithogenic and anthropogenic elements enter the upper ocean through atmospheric deposition (Park et al., 2006; Jo et al., 2007; Kim et al., 2011; Yan and Kim, 2015; Seo and Kim, 2020). The deep water of the East Sea is almost disconnected from the North Pacific Ocean, except through four shallow sills (<150 m). Thus, the East Sea is an ideal site to study the atmospheric inputs of various elements and their behaviors within a closed system.

In this study, we attempt to estimate the atmospheric input of seawater-dissolvable Pb in the East Sea using the inventory of dissolved Pb in the water column and the residence time of ^{210}Pb. The residence time of ^{210}Pb is calculated using the mass balance of the input terms (atmospheric deposition; ingrowth from ^{226}Ra in seawater) and the output terms (decay of ^{210}Pb; removal by sinking particles). For this mass balance estimation, we measured the distributions of total ^{210}Pb in seawater, dissolved Pb in seawater, and settling fluxes of ^{226}Ra and ^{210}Pb through 1000 m and 2000 m from sediment trap samples. In addition, we compile previously published ^{226}Ra and ^{210}Pb data including the Japan side for more accurate estimation.

MATERIALS AND METHODS

Sampling

For the measurements of total ^{210}Pb in seawater, sampling was conducted from April 6 to May 3 in 2015 on R/V *Akademik M.A. Lavrentyev* (**Figure 1**). Seawater samples (10 L, n = 29) were collected in high-density polyethylene (HDPE) bottles from Niskin samplers. The samples were acidified with 12 M HCl (pH < 2) within 1 hour to prevent ^{210}Pb from sorbing onto the bottles and then stored until analysis.

For the measurements of dissolved Pb in seawater, ultra-clean sampling was conducted from January 26 to February 2 in 2018 on R/V *Isabu* and from October 26 to November 22 in 2019 on R/V *Akademik Oparin*, respectively (**Figure 1**). We used PRISTINE ultra-clean CTD (UCC) and Teflon-coated Niskin-X samplers on the R/V *Isabu* and R/V *Akademik Oparin*, respectively. All procedures, including cleaning and sampling, followed the GEOTRACES protocol (Cutter et al., 2017). Seawater samples (125 mL, n = 64) were collected in pre-cleaned low-density polyethylene (LDPE) bottles from PRISTINE or Niskin-X samplers through pre-cleaned polyethersulfone capsule filters (0.2-μm pore size; AcroPak-200, Pall). The samples were acidified to pH ∼1.8 within 1 hour after sampling using 12 M HCl (ultra-high pure grade, ODLAB) and stored for laboratory analysis. Milli-Q water (18.2 MΩ, n = 15) was used as a procedural blank.

For ^{226}Ra and ^{210}Pb in sinking particles, the conical type sediment traps (MARK7G-21, McLane) were deployed at 1000 m and 2000 m depths from December 1998 to December 1999 (**Figure 1**). All sample cups were filled with $HgCl_2$ solutions before deployment to prevent the samples from bacterial degradation. After the recovery of the sediment traps, samples were kept below 4°C until they were transported to the land-based laboratory for further analysis.

Analytical Methods

The method for measuring the total phase of ^{210}Pb in seawater in this study was similar to that of previous studies (Kim and Kim, 2012; Seo et al., 2021). Briefly, all seawater samples for total ^{210}Pb were stored for more than 2 years to allow for the equilibrium between ^{210}Pb and ^{210}Po. ^{209}Po spike (1.5 dpm) and Fe^{3+} (50 mg) carrier were added to the samples and left to equilibrate for 24 hours. Ammonium hydroxide was used to adjust the pH to ∼8 for the co-precipitation of ^{210}Po and $Fe(OH)_3$. The supernatants were removed and then the precipitates were filtered. The precipitates were digested with a mixture solution of concentrated HNO_3 and HCl (1:1, v/v) to

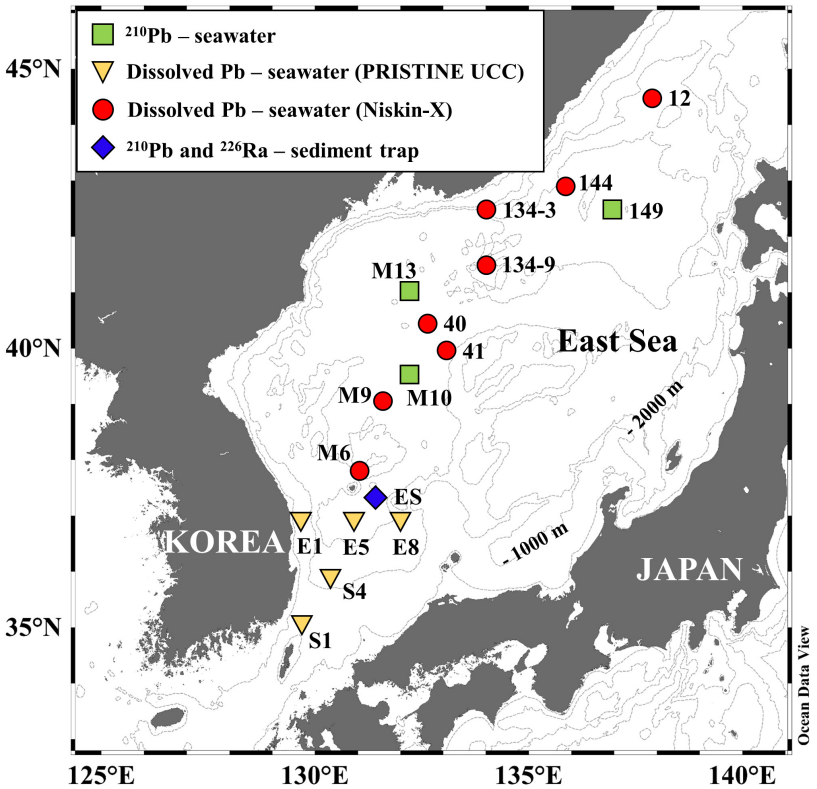

FIGURE 1 | Sampling locations for total ^{210}Pb and dissolved Pb in seawater and ^{210}Pb and ^{226}Ra in sinking particles.

remove any organic matter in the samples. The mixture solution was dried down and then re-dissolved in 50 mL of 0.5 M HCl. After adding ∼0.5 g of ascorbic acid to reduce Fe^{3+}, Po was plated onto a silver disk at a temperature of ∼80°C with stirring for 3 hours. ^{210}Po activities on the silver disks were counted by using alpha spectrometry (Alpha Analyst, Canberra). The measured counts were corrected for the background of the alpha spectrometry, decay of ^{210}Po during counting, recovery of ^{209}Po spike, decay of ^{210}Pb from sampling to plating, and the reagent blank (Church et al., 2012). The reagent blank for ^{210}Pb was 0.0175 ± 0.004 dpm (n = 5), which is comparable with those in Roca-Martí et al. (2021). The blank accounted for 1.1–4.6% (average: 2.7 ± 1.0%, n = 35) of the total ^{210}Pb in this study.

The concentrations of dissolved Pb were determined using an online pre-concentration system (seaFAST SP3; Elemental Scientific) coupled to a sector-field inductively coupled plasma mass spectrometry (ICP-MS; Element 2, Thermo Fisher Scientific). Approximately 10 mL of sample was buffered to pH ∼6.2 with a 4 M ammonium acetate buffer. The sample was loaded onto the seaFAST column filled with Nobias-chelate PA1 resin (200 μL), subsequently rinsed with a mixed solution of Milli-Q water and buffer to remove the salt. Then, Pb was eluted with 1.6 M HNO_3 (ultra-high pure grade, ODLAB). During the analysis, rhodium was used for an internal standard to correct the changes in ICP-MS sensitivity for each sample. The procedural blank and detection limit of this method was 3.9 pmol kg^{-1} and 2.8 pmol kg^{-1}, respectively. The accuracy of the measurement was determined by analyzing the certified reference materials (CASS-6 and NASS-7; National Research Council of Canada) and GEOTRACES reference standards (GSC: bottle number 97 and GSP: bottle number 36).

For ^{210}Pb and ^{226}Ra analyses in sinking particles, sediment trap samples were filtered through a 1 mm nylon mesh to separate swimmers and then freeze-dried. The freeze-dried samples were packed into gamma vials and sealed to avoid the loss of ^{222}Rn. After more than 3 weeks for the secular equilibrium between ^{226}Ra and its daughter (^{214}Pb and ^{214}Bi), the activities of ^{210}Pb and ^{226}Ra were measured using a gamma counter, with a high-purity germanium well detector (HPGe, Canberra), for the gamma-ray energy of each isotope (46.5 keV for ^{210}Pb; 351.9 keV for ^{214}Pb; 609.3 keV for ^{214}Bi). All analytical results are summarized in **Supplementary Tables 1–4**.

RESULTS

The vertical profiles of total ^{210}Pb in the East Sea showed the highest activities in the surface and decreased with depth, as observed in other major non-polar open oceans (Nozaki et al., 1980; Cochran et al., 1990; Kim, 2001; Rigaud et al., 2015; Tang et al., 2018; Horowitz et al., 2020; **Figure 2A**). The activities of total ^{210}Pb ranged from 9.3 to 16.4 dpm 100 L^{-1} (average: 12.8 ± 2.8 dpm 100 L^{-1}, n = 8) in the surface water (0–100 m) and decreased to a range from 4.2 to 6.6 dpm 100 L^{-1} (average:

5.0 ± 0.9 dpm 100 L^{-1}, n = 7) in the deep water (2500–3200 m). The activities of total ^{210}Pb in the surface water of the East Sea (0–100 m) were comparable with those in the North Pacific and North Atlantic Oceans, whereas the activities of total ^{210}Pb in the deep East Sea (2000 m) were approximately 4.8 and 2.2 times lower than those in the North Pacific and North Atlantic Oceans, respectively (Nozaki and Tsunogai, 1976; Nozaki et al., 1980; Rigaud et al., 2015).

The vertical profiles of dissolved Pb in the East Sea were similar to those of total ^{210}Pb, showing the surface maximum and decrease with depth, except at station E1 (**Figure 2B**). This distribution pattern differed from those in other open oceans, such as the central North Pacific, North Atlantic, and South Atlantic Oceans, which displayed a sub-surface maximum (Noble et al., 2015; Zurbrick et al., 2017, 2018; Schlosser et al., 2019; Zheng et al., 2019). The concentrations of dissolved Pb ranged from 45 to 107 pmol kg^{-1} (average: 73 ± 15 pmol kg^{-1}, n = 27) in the surface water (0–100 m) and decreased to a range from 4 to 15 pmol kg^{-1} (average: 8.5 ± 3.7 pmol kg^{-1}, n = 6) in the deep water (1500–2200 m). The concentrations of dissolved Pb in the surface water of the East Sea (0–100 m) were approximately 1.8 and 3.2 times higher than those in the North Pacific and North Atlantic Oceans, respectively. On the other hand, the concentrations of dissolved Pb in the deep East Sea (2000 m) were approximately 2.1 and 3.1 times lower than those in the North Pacific and North Atlantic Oceans, respectively (Noble et al., 2015; Zheng et al., 2019; Jiang et al., 2021). At station E1 (water depth: 190 m), the concentrations of Pb were ∼56 pmol kg^{-1} in the surface (0–100 m) and decreased to ∼26 pmol kg^{-1} in the sub-surface (100–150 m), followed by an increase to 38 pmol kg^{-1} near the bottom sediments.

The total particle flux through the sediment traps ranged from 0.09 to 1.27 g m^{-2} d^{-1} (average: 0.40 ± 0.23 g m^{-2} d^{-1}, n = 52) and 0.15 to 0.84 g m^{-2} d^{-1} (average: 0.36 ± 0.16 g m^{-2} d^{-1}, n = 57) at 1000 and 2000 m, respectively (**Figure 3A**). The total particle flux at 1000 m showed peaks in March (0.78 g m^{-2} d^{-1}), April (1.03 g m^{-2} d^{-1}), and November (1.27 g m^{-2} d^{-1}). At 2000 m, the seasonal variation of total particle flux was similar to that at 1000 m. The total particle flux at 1000 m in the East Sea was approximately 4 and 9 times higher than that in the North Pacific (Moored depth: 1004–1264 m; Tsunogai et al., 1982; Harada and Tsunogai, 1986b) and North Atlantic Oceans (Moored depth: 1500 m; Hong et al., 2013), respectively.

The sinking flux of particulate ^{210}Pb through the sediment traps ranged from 15 to 97 dpm m^{-2} d^{-1} (average: 46 ± 19 dpm m^{-2} d^{-1}, n = 52) and 17 to 115 dpm m^{-2} d^{-1} (average: 57 ± 20 dpm m^{-2} d^{-1}, n = 57) at 1000 and 2000 m, respectively (**Figure 3B**). The ^{210}Pb flux at 1000 m exhibited peaks in February (83 dpm m^{-2} d^{-1}), April (73 dpm m^{-2} d^{-1}), and November (97 dpm m^{-2} d^{-1}), similar to total particle flux, whereas 2000 m data showed peaks in February (107 dpm m^{-2} d^{-1}) and March (106 dpm m^{-2} d^{-1}). The sinking flux of particulate ^{210}Pb at 1000 m in the East Sea was approximately 5 and 3 times higher than that in the North Pacific (Moored depth: 1004–1264 m; Tsunogai et al., 1982; Harada and Tsunogai, 1986b) and North Atlantic Oceans (Moored depth: 1500 m; Hong et al., 2013), respectively. The activities of ^{226}Ra were ∼6% of ^{210}Pb in the sinking particles.

DISCUSSION

Budget of ^{210}Pb in the East Sea

The budget of ^{210}Pb in the East Sea is estimated using two different boxes of a steady-state scavenging model (0–1000 m or 0–2000 m). At steady state ($\partial A/\partial t = 0$), by neglecting advection and diffusion, the mass balance of ^{210}Pb can be calculated as follow:

$$\frac{\partial A_{Pb-210}}{\partial t} = \lambda_{Pb-210} \times \left(A_{Ra-226} - A_{Pb-210}\right) + F_{Atm} - k_{Pb-210}A_{Pb-210} = 0 \quad (1)$$

where λ, F_{Atm}, k, and A represent the decay constant of ^{210}Pb (y^{-1}), atmospheric depositional flux of ^{210}Pb (dpm cm^{-2} y^{-1}), first-order scavenging rate constant (y^{-1}), and inventory of each radionuclide (dpm cm^{-2}) in the 0–1000 m and 0–2000 m, respectively. For the inventory of total ^{210}Pb, we compile our measured data with previously published data from the East Sea (Nozaki et al., 1973; Kim and Kim, 2012; Seo et al., 2021; this study). The inventory of ^{226}Ra in the East Sea is from the published results (Harada and Tsunogai, 1986a; Inoue et al., 2015). The first-order scavenging flux ($k_{Pb-210}A_{Pb-210}$) is measured using the $^{210}Pb_{ex}$ flux through the sediment traps. The sediment trap samples were not available in several periods (November 11–December 11 in 1999 at 1000 m; December 6–13 in 1998 and April 25–29 in 1999 at 2000 m). In order to estimate the annual $^{210}Pb_{ex}$ flux, we interpolate the $^{210}Pb_{ex}$ flux for the missing-sample periods using the significant correlation between the monthly average $^{210}Pb_{ex}$ fluxes at 1000 m and 2000 m (r^2 = 0.85; **Supplementary Figure 1**). In addition, we note that sediment trap samples of this study were obtained 16 years before the seawater sampling for ^{210}Pb. However, the activities of ^{210}Pb in seawater were similar from the 1970s to the 2010s in the East Sea (Nozaki et al., 1973; Kim and Kim, 2012; Seo et al., 2021; this study). Thus, we assume that there was no temporal change in ^{210}Pb in the East Sea over a few decades.

In Eq. (1), the only unknown term is the atmospheric input of ^{210}Pb into the ocean (F_{Atm}). The atmospheric input of ^{210}Pb should be balanced by the *in situ* production from ^{226}Ra, *in situ* decay of ^{210}Pb, and settling flux to the deeper layer (**Figure 4**). Then, the atmospheric input of ^{210}Pb is calculated to be 1.37 ± 0.22 and 1.55 ± 0.27 dpm cm^{-2} y^{-1} according to the water boxes of 0–1000 m and 0–2000 m, respectively. The results are consistent despite the different depths of both boxes, indicating no significant effect of the lateral transport of total ^{210}Pb. The atmospheric input of ^{210}Pb in the East Sea (1.46 ± 0.25 dpm cm^{-2} y^{-1}) is similar to the average of previously reported values (1.64 ± 1.10 dpm cm^{-2} y^{-1}) in this sea based on the land-based measurements or the numerical modeling, which showed large variations depending on the measurement sites and periods (0.44–4.40 dpm cm^{-2} y^{-1}; Tokieda et al., 1996;

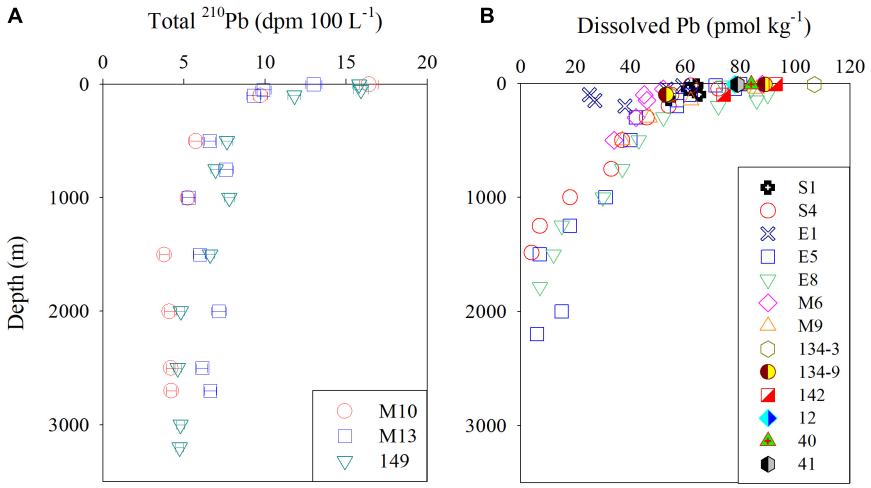

FIGURE 2 | Vertical profiles of **(A)** total ^{210}Pb (dpm 100 L^{-1}) and **(B)** dissolved Pb (pmol kg^{-1}) in the East Sea.

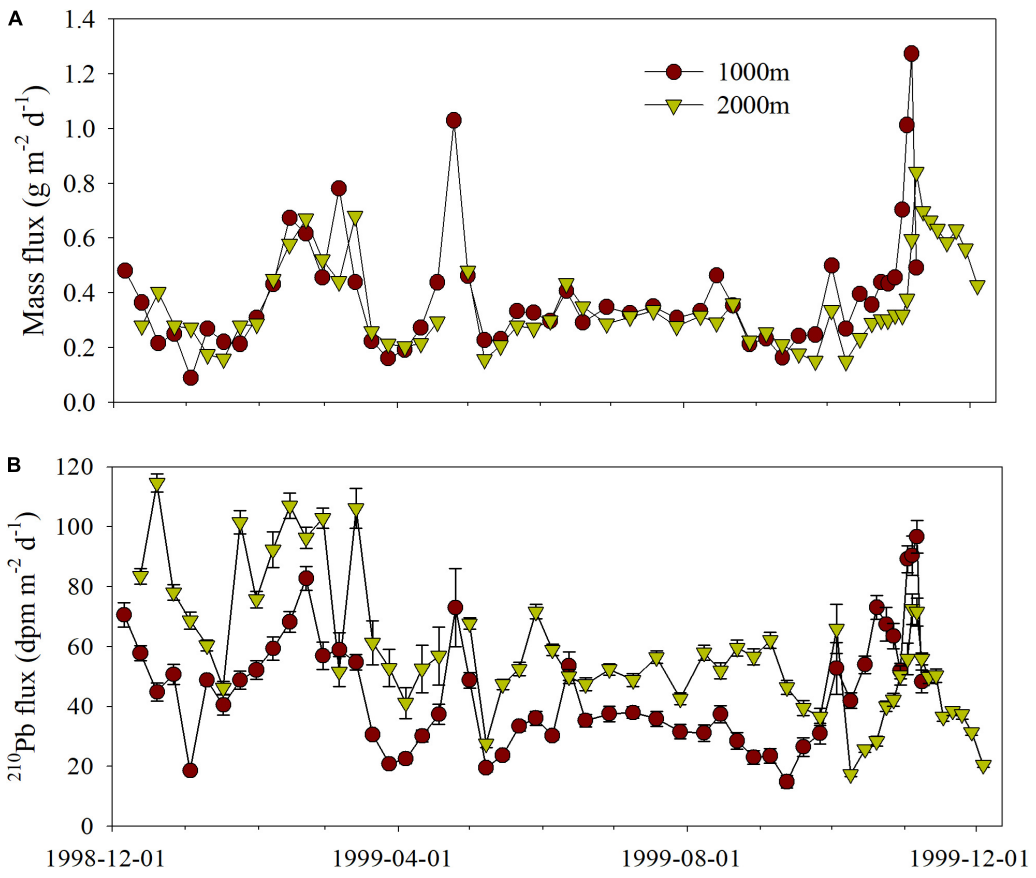

FIGURE 3 | One-year time series data (December 1998 to December 1999) of **(A)** total particulate flux (g m^{-2} d^{-1}) and **(B)** ^{210}Pb (dpm m^{-2} d^{-1}) flux in the sinking particles.

Henderson and Maier-Reimer, 2002; Hirose et al., 2004; Yi et al., 2007; Akata et al., 2008; Du et al., 2008, 2015; Tateda and Iwao, 2008; **Table 1**). It is reasonable to assume that the atmospheric input of ^{210}Pb calculated from the ^{210}Pb budget in the ocean represents the actual atmospheric flux over the annual to decadal time scales. The atmospheric ^{210}Pb flux in the East Sea is 2–4 times higher than that in the major open oceans, such as the North Pacific (0.22–0.30 dpm cm^{-2} y^{-1}; Turekian, 1989),

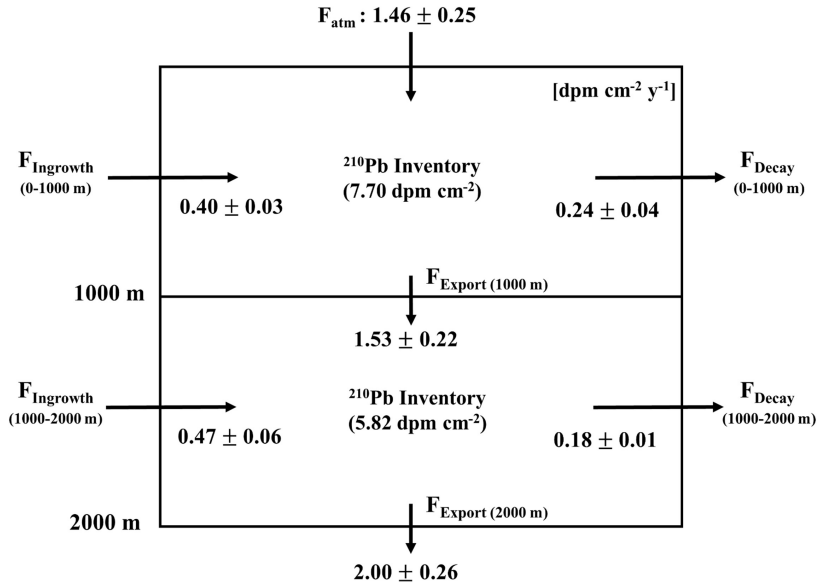

FIGURE 4 | A schematic box model accounting for the ingrowth, decay, export, and atmospheric flux of ^{210}Pb in the East Sea (dpm cm^{-2} y^{-1}).

TABLE 1 | Comparison of atmospheric depositional fluxes of ^{210}Pb (dpm cm^{-2} y^{-1}) around the East Sea.

Study area	Lat.	Long.	Collection period	Method	^{210}Pb flux (dpm cm^{-2} y^{-1})		References
					Average	Range	
Rokkasho, Japan	41.0°N	141.4°E	July 2000–March 2006	Bulk deposition (no leaching)	4.38	1.10–55.3	Akata et al., 2008
Tsukuba, Japan	36.1°N	140.1°E	January 2000–December 2001	Bulk deposition (no leaching)	1.10	0.62–2.26	Hirose et al., 2004
Nagasaki, Japan	32.8°N	129.8°E	January 2000–December 2000		1.39	0.07–5.62	
Odawa Bay, Japan	35.2°N	139.6°E	September 1997–August 1998	Bulk deposition (leaching with HNO_3)	0.47	0.07–2.04	Tateda and Iwao, 2008
Tsuyazaki, Japan	33.8°N	130.5°E			1.17	0.26–3.47	
Akajima, Japan	26.2°N	127.3°E			0.51	0.04–2.08	
Hakodate, Japan	41.8°N	140.7°E	January 1990–June 1991	Wet deposition (no leaching)	1.61	0.22–3.69	Tokieda et al., 1996
Xiamen, China	24.4°N	118.1°E	March 2004–April 2005	Bulk deposition (leaching with 0.2 M HCl)	1.13	0.07–1.86	Yi et al., 2007
Shanghai, China	31.2°N	121.4°E	November 2005–October 2006	Bulk deposition (leaching with HNO_3)	2.88	0.66–7.30	Du et al., 2008
Shanghai, China	31.2°N	121.4°E	December 2005–December 2013	Bulk deposition (leaching with 0.2 M HNO_3)	2.30	0.51–5.99	Du et al., 2015
East Sea				Atmospheric model (^{222}Rn)	0.99–1.39		Henderson and Maier-Reimer, 2002
East Sea				Water column mass balance	1.37–1.55		This study

equatorial Pacific (0.11–0.51 dpm cm^{-2} y^{-1}; Murray et al., 2005), North Atlantic (0.40–0.69 dpm cm^{-2} y^{-1}; Turekian et al., 1983; Kim et al., 1999), and Indian Oceans (0.73 dpm cm^{-2} y^{-1}; Sarin et al., 1999), respectively. However, the atmospheric input of ^{210}Pb in the East Sea approaches the upper limit of that in the corresponding latitudinal belt of global fallout curve (average: 0.96 ± 0.58 dpm cm^{-2} y^{-1}, 30–40°N, Baskaran, 2011). This higher flux in the study region is known to be due the elevated emanation of ^{222}Rn from the Asian continent (Baskaran, 2011; Zhang et al., 2021).

The residence time of ^{210}Pb in the water column can be calculated using Eq. (2):

$$\tau = \frac{1}{k_{Pb-210}} = \frac{A_{Pb-210}}{A_{Ra-226}\lambda_{Pb-210} - A_{Pb-210}\lambda_{Pb-210} + F_{Atm}} \quad (2)$$

where τ is the residence time of total ^{210}Pb. The residence times of total ^{210}Pb are estimated to be 4.8 ± 1.2 years and 7.1 ± 1.6 years in the 0–1000 m and 0–2000 m, respectively. The calculated result in this study (7 years, 0–2000 m) is approximately 2.3 times lower

TABLE 2 | Comparison of atmospheric depositional fluxes of Pb (nmol cm^{-2} y^{-1}) around the East Sea.

Study area	Fraction	Collection period	Pb flux (nmol cm^{-2} y^{-1})	References
Japan (10 sites)	Wet deposition (leaching with 0.3 M HNO_3)	December 2003–November 2004	2.26 ± 1.50	Sakata et al., 2006
Tokyo Bay	Wet deposition (leaching with 0.3 M HNO_3)	December 2003–November 2005	3.14 ± 1.28	Sakata et al., 2008
Sea coast of Japan (Noshiro)	Wet deposition (leaching with 0.3 M HNO_3)	December 2002–March 2006	4.34 ± 1.42	Sakata and Asakura, 2009
Sea coast of Japan (Nakanoto)			4.82 ± 0.95	
Sea coast of Japan (Matsuura)			3.32 ± 0.44	
East Sea	Actual dissolvable fraction into the seawater	–	0.98 ± 0.28	This study

than that in the Nozaki et al. (1973) (15 years; 0–2000 m) from the same region. The different residence time of ^{210}Pb by Nozaki et al. (1973) is associated with the different atmospheric input term. Nozaki et al. (1973) assumed that approximately 2.0 dpm cm^{-2} y^{-1} of ^{210}Pb entered the East Sea from the atmosphere, and only a quarter of that (0.5 dpm cm^{-2} y^{-1}) was transported into the deeper layer. It resulted in the net removal flux of ^{210}Pb at 2000 m to be 0.8 dpm cm^{-2} y^{-1}, which is 2.5 times lower than the measured flux from the sediment trap (moored depth: 2000 m) (2.0 dpm cm^{-2} y^{-1}; this study) or sedimentation rates in this region (water depth: ∼2200 m) (1.79 to 2.70 dpm cm^{-2} y^{-1}; Hong et al., 1997; Hong et al., 1999). Thus, our estimated residence time of ^{210}Pb in the East Sea, which is much shorter than the previous estimation, appears to be more reliable. The residence time of ^{210}Pb in the East Sea is 1.5–15 times lower than that in the major oceans, such as the North Pacific (54 years, ∼1800–4000 m, Craig et al., 1973; 96 years, ∼1000–4000 m, Nozaki and Tsunogai, 1976), southeastern Pacific (95 years, ∼0–3700 m, Niedermiller and Baskaran, 2019), North Atlantic (15–22 years, ∼0–3000 m, Cochran et al., 1990), and Indian Oceans (10–15 years, ∼500–4000 m, Obata et al., 2004). The shorter residence time of ^{210}Pb in the water column of this sea seems to result in the lower concentrations of ^{210}Pb and Pb in the deep ocean, relative to other major oceans, although their atmospheric input fluxes were higher (e.g., Akata et al., 2008; Sakata and Asakura, 2009; Du et al., 2015). This was also evidenced by the fractionations of rare earth elements (Seo and Kim, 2020). The higher removal rates have been attributed to higher fluxes of sinking particles, which mainly consist of lithogenic materials and opal (>80%) (Kim et al., 2020).

Atmospheric Input of Seawater-Dissolvable Pb

In order to calculate the atmospheric input of seawater-dissolvable Pb in the East Sea, we apply the residence time of dissolved ^{210}Pb in this study. Assuming that dissolved ^{210}Pb is about 80–90% of total ^{210}Pb in the East Sea (Kim and Kim, 2012), the residence times of dissolved ^{210}Pb in this sea are estimated to be 4.0 ± 1.0 years and 5.8 ± 1.3 years in the 0–1000 m and 0–2000 m, respectively. The average annual atmospheric depositional flux of seawater-dissolvable Pb can be obtained by dividing the inventory of dissolved Pb by the residence time of dissolved ^{210}Pb. The Pb data of station E1 is excluded from this calculation because of the distinctly low concentrations in the 100–150 m layer, which might be due to boundary scavenging.

The atmospheric input of seawater-dissolvable Pb is calculated to be 0.98 ± 0.28 nmol cm^{-2} y^{-1}. Although Pb can be introduced into the East Sea from the adjacent continental shelf, including the East China Sea and the Yellow Sea, we exclude this source since the concentrations of dissolved Pb (0–100 m) in the southern East Sea (stations S1, S4, E5, and E8; ∼69 pmol kg^{-1}) were lower than those in the northern East Sea (stations M9, 40, 41, 134-3, 134-9, 144, and 12; ∼78 pmol kg^{-1}). The atmospheric input of seawater-dissolvable Pb in the East Sea is distinctively higher than wet deposition of Pb in the remote oceans, including the North Pacific (0.05–0.08 nmol cm^{-2} y^{-1}; Settle et al., 1982; Duce et al., 1991), North Atlantic (0.03–0.46 nmol cm^{-2} y^{-1}; Duce et al., 1991; Helmers and Schrems, 1995; Kim et al., 1999), and North Indian Oceans (0.01 nmol cm^{-2} y^{-1}; Duce et al., 1991). Our calculated Pb flux is approximately 25% of the previously published fluxes around this region, which used the leaching method with nitric acid for precipitation samples collected on land (Sakata et al., 2006, 2008; Sakata and Asakura, 2009; **Table 2**). Diluted nitric or hydrochloric acid has been widely used to desorb Pb from the particles in precipitation. We believe that the leaching method could overestimate the atmospheric depositional flux of seawater-dissolvable Pb since the much lower pH in this process than the actual pH of seawater can affect the solubility of Pb (Chester et al., 2000; Martín-Torre et al., 2015). Our results suggest that the application of ^{210}Pb provides a useful tool to estimate the flux of actual seawater-dissolvable Pb in the ocean. However, the estimated flux of seawater-dissolvable Pb in this study cannot distinguish the relative contribution of different origins of Pb (leaded gasoline, coal burning, and dust). Thus, future studies are necessary to determine the solubility of atmospheric Pb in the ocean according to its origins.

CONCLUSION

The budget of ^{210}Pb in the East Sea is determined by measuring the activities of ^{210}Pb in seawater and sinking particles. Based on the different depths (1000 m or 2000 m) of the scavenging

box model, the atmospheric input of ^{210}Pb is estimated to be 1.46 ± 0.25 dpm cm^{-2} y^{-1}. Based on this atmospheric input of ^{210}Pb, the residence time of ^{210}Pb in the East Sea (0–2000 m) is calculated to be 7.1 ± 1.6 years, which is an order of magnitude lower than that in the major open oceans due to the efficient Pb removal in the East Sea. Combining this residence time and the concentrations of dissolved Pb, the atmospheric input of seawater-dissolvable Pb is calculated to be 0.98 ± 0.28 nmol cm^{-2} y^{-1}, which is ∼25% lower than the previous wet deposition results in this region. Thus, our results suggest that our approach, measuring the flux of seawater dissolvable Pb using the ^{210}Pb budget in the ocean, can be successfully used for other major oceans.

DATA AVAILABILITY STATEMENT

The original contributions presented in the study are included in the article/**Supplementary Material**, further inquiries can be directed to the corresponding author.

AUTHOR CONTRIBUTIONS

GK conceptualized the study. HS, Y-IK, and IK performed the field sampling and analyses. HS and GK interpreted the data and wrote the manuscript. All authors contributed to the final version of the manuscript.

FUNDING

This research was supported by the project titled "Deep Water Circulation and Material Cycling in the East Sea (20160400)," funded by the Ministry of Oceans and Fisheries, South Korea, and the National Research Foundation of Korea (NRF) grant funded by the Korean government (MSIT; 2018R1A2B3001147).

ACKNOWLEDGMENTS

We thank the crew members of R/V *Akademik M.A. Lavrentyev* and R/V *Isabu* for helping with the sampling. We also thank all lab members for their assistance.

SUPPLEMENTARY MATERIAL

The Supplementary Material for this article can be found online at: https://www.frontiersin.org/articles/10.3389/fmars.2021.756076/full#supplementary-material

REFERENCES

Akata, N., Kawabata, H., Hasegawa, H., Sato, T., Chikuchi, Y., Kondo, K., et al. (2008). Total deposition velocities and scavenging ratios of ^{7}Be and ^{210}Pb at Rokkasho, Japan. *J. Radioanal. Nucl. Chem.* 277, 347–355. doi: 10.1007/s10967-007-7095-1

Anderson, R., Fleisher, M., Biscaye, P., Kumar, N., Dittrich, B., Kubik, P., et al. (1994). Anomalous boundary scavenging in the Middle Atlantic Bight: evidence from ^{230}Th, ^{231}Pa, ^{10}Be and ^{210}Pb. *Deep Sea Res. II* 41, 537–561. doi: 10.1016/0967-0645(94)90034-5

Bacon, M., Spencer, D., and Brewer, P. (1976). ^{210}Pb/^{226}Ra and ^{210}Po/^{210}Pb disequilibria in seawater and suspended particulate matter. *Earth Planet. Sci. Lett.* 32, 277–296. doi: 10.1016/0012-821X(76)90068-6

Balkanski, Y. J., Jacob, D. J., Gardner, G. M., Graustein, W. C., and Turekian, K. K. (1993). Transport and residence times of tropospheric aerosols inferred from a global three-dimensional simulation of ^{210}Pb. *J. Geophys. Res. Atmos.* 98, 20573–20586. doi: 10.1029/93JD02456

Baskaran, M. (2011). Po-210 and Pb-210 as atmospheric tracers and global atmospheric Pb-210 fallout: a review. *J. Environ. Radioact.* 102, 500–513. doi: 10.1016/j.jenvrad.2010.10.007

Baskaran, M., and Krupp, K. (2021). Novel Application of ^{210}Po-^{210}Pb disequilibria to date snow, melt pond, ice core and ice-rafted sediments in the Arctic Ocean. *Front. Mar. Sci.* 8:892. doi: 10.3389/fmars.2021.692631

Boyle, E., Chapnick, S., Shen, G., and Bacon, M. (1986). Temporal variability of lead in the western North Atlantic. *J. Geophys. Res. Oceans* 91, 8573–8593. doi: 10.1029/JC091iC07p08573

Chester, R., Nimmo, M., Fones, G., Keyse, S., and Zhang, J. (2000). The solubility of Pb in coastal marine rainwaters: pH-dependent relationships. *Atmos. Environ.* 34, 3875–3887. doi: 10.1016/S1352-2310(00)00177-1

Church, T., Rigaud, S., Baskaran, M., Kumar, A., Friedrich, J., Masque, P., et al. (2012). Intercalibration studies of ^{210}Po and ^{210}Pb in dissolved and particulate seawater samples. *Limnol. Oceanogr. Methods* 10, 776–789. doi: 10.4319/lom.2012.10.776

Cochran, J. K., McKibbin-Vaughan, T., Dornblaser, M. M., Hirschberg, D., Livingston, H. D., and Buesseler, K. O. (1990). ^{210}Pb scavenging in the North Atlantic and North Pacific oceans. *Earth Planet. Sci. Lett.* 97, 332–352. doi: 10.1016/0012-821X(90)90050-8

Craig, H., Krishnaswami, S., and Somayajulu, B. (1973). ^{210}Pb–^{226}Ra: radioactive disequilibrium in the deep sea. *Earth Planet. Sci. Lett.* 17, 295–305. doi: 10.1016/0012-821X(73)90194-5

Cutter, G., Casciotti, K., Croot, P., Geibert, W., Heimbürger, L.-E., Lohan, M., et al. (2017). *Sampling and Sample-handling Protocols for GEOTRACES Cruises. Version 3*. Toulouse: GEOTRACES International Project Office.

Du, J., Du, J., Baskaran, M., Bi, Q., Huang, D., and Jiang, Y. (2015). Temporal variations of atmospheric depositional fluxes of ^{7}Be and ^{210}Pb over 8 years (2006–2013) at Shanghai, China, and synthesis of global fallout data. *J. Geophys. Res. Atmos.* 120, 4323–4339. doi: 10.1002/2014JD022807

Du, J., Zhang, J., and Wu, Y. (2008). Deposition patterns of atmospheric ^{7}Be and ^{210}Pb in coast of East China sea, Shanghai, China. *Atmos. Environ.* 42, 5101–5109. doi: 10.1016/j.atmosenv.2008.02.007

Duce, R., Liss, P., Merrill, J., Atlas, E., Buat-Menard, P., Hicks, B., et al. (1991). The atmospheric input of trace species to the world ocean. *Global Biogeochem. Cycles* 5, 193–259. doi: 10.1029/91GB01778

Elsässer, C., Wagenbach, D., Weller, R., Auer, M., Wallner, A., and Christl, M. (2011). Continuous 25-yr aerosol records at coastal Antarctica: part 2: variability of the radionuclides ^{7}Be, ^{10}Be and ^{210}Pb. *Tellus B Chem. Phys. Meteorol.* 63, 920–934.

Feichter, J., Brost, R., and Heimann, M. (1991). Three-dimensional modeling of the concentration and deposition of ^{210}Pb aerosols. *J. Geophys. Res. Atmos.* 96, 22447–22460. doi: 10.1029/91JD02354

Gamo, T. (1999). Global warming may have slowed down the deep conveyor belt of a marginal sea of the northwestern Pacific: Japan sea. *Geophys. Res. Lett.* 26, 3137–3140. doi: 10.1029/1999GL002341

Harada, K., and Tsunogai, S. (1986a). ^{226}Ra in the Japan sea and the residence time of the Japan sea water. *Earth Planet. Sci. Lett.* 77, 236–244. doi: 10.1016/0012-821X(86)90164-0

Harada, K., and Tsunogai, S. (1986b). Fluxes of ^{234}Th, ^{210}Po and ^{210}Pb determined by sediment trap experiments in pelagic oceans. *J. Oceanogr.* 42 192–200. doi: 10.1007/BF02109353

Helmers, E., and Schrems, O. (1995). Wet deposition of metals to the tropical North and the South Atlantic ocean. *Atmos. Environ.* 29, 2475–2484. doi: 10.1016/1352-2310(95)00159-V

Henderson, G. M., and Maier-Reimer, E. (2002). Advection and removal of ^{210}Pb and stable Pb isotopes in the oceans: a general circulation model study. *Geochim. Cosmochim. Acta* 66, 257–272. doi: 10.1016/S0016-7037(01)00779-7

Hirose, K., Honda, T., Yagishita, S., Igarashi, Y., and Aoyama, M. (2004). Deposition behaviors of ^{210}Pb, ^{7}Be and thorium isotopes observed in Tsukuba and Nagasaki, Japan. *Atmos. Environ.* 38, 6601–6608. doi: 10.1016/j.atmosenv.2004.08.012

Hong, G., Baskaran, M., Church, T. M., and Conte, M. (2013). Scavenging, cycling and removal fluxes of ^{210}Po and ^{210}Pb at the Bermuda time-series study site. *Deep Sea Res. II* 93, 108–118. doi: 10.1016/j.dsr2.2013.01.005

Hong, G., Kim, S., Chung, C., Kang, D.-J., Shin, D.-H., Lee, H., et al. (1997). ^{210}Pb-derived sediment accumulation rates in the southwestern East Sea (Sea of Japan). *Geo Mar. Lett.* 17, 126–132. doi: 10.1007/s003670050017

Hong, G.-H., Lee, S.-H., Kim, S.-H., Chung, C.-S., and Baskaran, M. (1999). Sedimentary fluxes of ^{90}Sr, ^{137}Cs, ^{239,240}Pu and ^{210}Pb in the East Sea (Sea of Japan). *Sci. Total Environ.* 237, 225–240. doi: 10.1016/S0048-9697(99)00138-2

Horowitz, E. J., Cochran, J. K., Bacon, M. P., and Hirschberg, D. J. (2020). ^{210}Po and ^{210}Pb distributions during a phytoplankton bloom in the North Atlantic: implications for POC export. *Deep Sea Res. I* 164:103339. doi: 10.1016/j.dsr.2020.103339

Ichiye, T. (1984). *Some Problems of Circulation and Hydrography of the Japan Sea and the Tsushima Current, Elsevier oceanography series*. Amsterdam: Elsevier, 15–54. doi: 10.1016/S0422-9894(08)70289-7

Inoue, M., Minakawa, M., Yoshida, K., Nakano, Y., Kofuji, H., Nagao, S., et al. (2015). Vertical profiles of ^{228}Ra and ^{226}Ra activities in the Sea of Japan and their implications on water circulation. *J. Radioanal. Nucl. Chem.* 303, 1309–1312. doi: 10.1007/s10967-014-3492-4

Jenkins, W. J. (1980). Tritium and 3He in the Sargasso Sea. *J. Mar. Res.* 38, 553–569.

Jiang, S., Zhang, J., Zhou, H., Xue, Y., and Zheng, W. (2021). Concentration of dissolved lead in the upper Northwestern Pacific Ocean. *Chem. Geol.* 577:120275. doi: 10.1016/j.chemgeo.2021.120275

Jo, C. O., Lee, J. Y., Park, K. A., Kim, Y. H., and Kim, K. R. (2007). Asian dust initiated early spring bloom in the northern East/Japan Sea. *Geophys. Res. Lett.* 34:L05602. doi: 10.1029/2006GL027395

Kim, G. (2001). Large deficiency of polonium in the oligotrophic ocean's interior. *Earth Planet. Sci. Lett.* 192, 15–21. doi: 10.1016/S0012-821X(01)00431-9

Kim, G., Alleman, L. Y., and Church, T. M. (1999). Atmospheric depositional fluxes of trace elements, ^{210}Pb, and ^{7}Be to the Sargasso sea. *Global Biogeochem. Cycles* 13, 1183–1192. doi: 10.1029/1999GB900071

Kim, K., Kim, K. R., Min, D. H., Volkov, Y., Yoon, J. H., and Takematsu, M. (2001). Warming and structural changes in the East (Japan) Sea: a clue to future changes in global oceans? *Geophys. Res. Lett.* 28, 3293–3296. doi: 10.1029/2001GL013078

Kim, M., Kim, Y.-I., Hwang, J., Choi, K. Y., Kim, C. J., Ryu, Y., et al. (2020). Influence of sediment resuspension on the biological pump of the Southwestern East Sea (Japan Sea). *Front. Earth Sci.* 8:144. doi: 10.3389/feart.2020.00144

Kim, T.-H., and Kim, G. (2012). Important role of colloids in the cycling of ^{210}Po and ^{210}Pb in the ocean: results from the East/Japan Sea. *Geochim. Cosmochim. Acta* 95, 134–142. doi: 10.1016/j.gca.2012.07.029

Kim, T.-W., Lee, K., Najjar, R. G., Jeong, H.-D., and Jeong, H. J. (2011). Increasing N abundance in the northwestern Pacific Ocean due to atmospheric nitrogen deposition. *Science* 334, 505–509. doi: 10.1126/science.1206583

Kumamoto, Y. I., Yoneda, M., Shibata, Y., Kume, H., Tanaka, A., Uehiro, T., et al. (1998). Direct observation of the rapid turnover of the Japan Sea bottom water by means of AMS radiocarbon measurement. *Geophys. Res. Lett.* 25, 651–654. doi: 10.1029/98GL00359

Martín-Torre, M. C., Payán, M. C., Verbinnen, B., Coz, A., Ruiz, G., Vandecasteele, C., et al. (2015). Metal release from contaminated estuarine sediment under pH changes in the marine environment. *Arch. Environ. Contam. Toxicol.* 68, 577–587. doi: 10.1007/s00244-015-0133-z

Murray, J. W., Paul, B., Dunne, J. P., and Chapin, T. (2005). ^{234}Th, ^{210}Pb, ^{210}Po and stable Pb in the central equatorial Pacific: tracers for particle cycling. *Deep Sea Res. I* 52, 2109–2139. doi: 10.1016/j.dsr.2005.06.016

Niedermiller, J., and Baskaran, M. (2019). Comparison of the scavenging intensity, remineralization and residence time of ^{210}Po and ^{210}Pb at key zones (biotic, sediment-water and hydrothermal) along the East Pacific GEOTRACES transect. *J. Environ. Radioact.* 198, 165–188. doi: 10.1016/j.jenvrad.2018.12.016

Noble, A. E., Echegoyen-Sanz, Y., Boyle, E. A., Ohnemus, D. C., Lam, P. J., Kayser, R., et al. (2015). Dynamic variability of dissolved Pb and Pb isotope composition from the US North Atlantic GEOTRACES transect. *Deep Sea Res. II* 116, 208–225. doi: 10.1016/j.dsr2.2014.11.011

Nozaki, Y., Dobashi, F., Kato, Y., and Yamamoto, Y. (1998). Distribution of Ra isotopes and the ^{210}Pb and ^{210}Po balance in surface seawaters of the mid Northern Hemisphere. *Deep Sea Res. I* 45, 1263–1284. doi: 10.1016/S0967-0637(98)00016-8

Nozaki, Y., Thomson, J., and Turekian, K. (1976). The distribution of ^{210}Pb and ^{210}Po in the surface waters of the Pacific Ocean. *Earth Planet. Sci. Lett.* 32, 304–312. doi: 10.1016/0012-821X(76)90070-4

Nozaki, Y., and Tsunogai, S. (1973). Lead-210 in the North Pacific and the transport of terrestrial material through the atmosphere. *Earth Planet. Sci. Lett.* 20, 88–92. doi: 10.1016/0012-821X(73)90143-X

Nozaki, Y., and Tsunogai, S. (1976). ^{226}Ra, ^{210}Pb and ^{210}Po disequilibria in the western North Pacific. *Earth Planet. Sci. Lett.* 32, 313–321. doi: 10.1016/0012-821X(76)90071-6

Nozaki, Y., Tsunogai, S., and Nishimura, M. (1973). Lead-210 in the Japan Sea. *J. Oceanogr.* 29, 251–256.

Nozaki, Y., Turekian, K., and Von Damm, K. (1980). ^{210}Pb in GEOSECS water profiles from the North Pacific. *Earth Planet. Sci. Lett.* 49, 393–400. doi: 10.1016/0012-821X(80)90081-3

Obata, H., Nozaki, Y., Alibo, D. S., and Yamamoto, Y. (2004). Dissolved Al, In, and Ce in the eastern Indian Ocean and the Southeast Asian seas in comparison with the radionuclides ^{210}Pb and ^{210}Po. *Geochim. Cosmochim. Acta* 68, 1035–1048. doi: 10.1016/j.gca.2003.07.021

Park, G. H., Lee, K., Tishchenko, P., Min, D. H., Warner, M. J., Talley, L. D., et al. (2006). Large accumulation of anthropogenic CO_2 in the East (Japan) Sea and its significant impact on carbonate chemistry. *Global Biogeochem. Cycles* 20:GB4013. doi: 10.1029/2005GB002676

Persson, B. R., and Holm, E. (2014). ^{7}Be, ^{210}Pb, and ^{210}Po in the surface air from the Arctic to Antarctica. *J. Environ. Radioact.* 138, 364–374.

Rengarajan, R., and Sarin, M. (2004). Atmospheric deposition fluxes of ^{7}Be,^{210}Pb and chemical species to the Arabian Sea and Bay of Bengal. *Indian J. Mar. Sci.* 33, 56–64.

Rigaud, S., Stewart, G., Baskaran, M., Marsan, D., and Church, T. (2015). ^{210}Po and ^{210}Pb distribution, dissolved-particulate exchange rates, and particulate export along the North Atlantic US GEOTRACES GA03 section. *Deep Sea Res. II* 116, 60–78. doi: 10.1016/j.dsr2.2014.11.003

Roca-Martí, M., Puigcorbé, V., Castrillejo, M., Casacuberta, N., Garcia-Orellana, J., Cochran, J. K., et al. (2021). Quantifying 210Po/210Pb disequilibrium in seawater: a comparison of two precipitation methods with differing results. *Front. Mar. Sci.* 8:684484. doi: 10.3389/fmars.2021.684484

Sakata, M., and Asakura, K. (2009). Factors contributing to seasonal variations in wet deposition fluxes of trace elements at sites along Japan Sea coast. *Atmos. Environ.* 43, 3867–3875. doi: 10.1016/j.atmosenv.2009.05.001

Sakata, M., Marumoto, K., Narukawa, M., and Asakura, K. (2006). Regional variations in wet and dry deposition fluxes of trace elements in Japan. *Atmos. Environ.* 40, 521–531. doi: 10.1016/j.atmosenv.2005.09.066

Sakata, M., Tani, Y., and Takagi, T. (2008). Wet and dry deposition fluxes of trace elements in Tokyo Bay. *Atmos. Environ.* 42, 5913–5922. doi: 10.1016/j.atmosenv.2008.03.027

Sarin, M., Rengarajan, R., and Krishnaswami, S. (1999). Aerosol NO-3 and ^{210}Pb distribution over the central-eastern Arabian Sea and their air'sea deposition fluxes. *Tellus B* 51, 749–758. doi: 10.3402/tellusb.v51i4.16480

Schlosser, C., Karstensen, J., and Woodward, E. M. S. (2019). Distribution of dissolved and leachable particulate Pb in the water column along the GEOTRACES section GA10 in the South Atlantic. *Deep Sea Res. I* 148, 132–142. doi: 10.1016/j.dsr.2019.05.001

Seo, H., Joung, D., and Kim, G. (2021). Contrasting behaviors of ^{210}Pb and ^{210}Po in the productive shelf water versus the oligotrophic water. *Front. Mar. Sci.* 8:772. doi: 10.3389/fmars.2021.701441

Seo, H., and Kim, G. (2020). Rare earth elements in the East Sea (Japan Sea): distributions, behaviors, and applications. *Geochim. Cosmochim. Acta* 286, 19–28. doi: 10.1016/j.gca.2020.07.016

Settle, D., Patterson, C., Turekian, K., and Cochran, J. (1982). Lead precipitation fluxes at tropical oceanic sites determined from ^{210}Pb measurements. *J. Geophys. Res. Oceans* 87, 1239–1245. doi: 10.1029/JC087iC02p01239

Shen, G. T., and Boyle, E. A. (1988). Thermocline ventilation of anthropogenic lead in the western North Atlantic. *J. Geophys. Res. Oceans* 93, 15715–15732. doi: 10.1029/JC093iC12p15715

Sherrell, R. M., Boyle, E. A., and Hamelin, B. (1992). Isotopic equilibration between dissolved and suspended particulate lead in the Atlantic Ocean: evidence from ^{210}Pb and stable Pb isotopes. *J. Geophys. Res. Oceans* 97, 11257–11268. doi: 10.1029/92JC00759

Tang, Y., Castrillejo, M., Roca-Martí, M., Masqué, P., Lemaitre, N., and Stewart, G. (2018). Distributions of total and size-fractionated particulate ^{210}Po and ^{210}Pb activities along the North Atlantic GEOTRACES GA01 transect: GEOVIDE cruise. *Biogeosciences* 15, 5437–5453. doi: 10.5194/bg-15-5437-2018

Tateda, Y., and Iwao, K. (2008). High ^{210}Po atmospheric deposition flux in the subtropical coastal area of Japan. *J. Environ. Radioact.* 99, 98–108. doi: 10.1016/j.jenvrad.2007.07.005

Tokieda, T., Yamanaka, K., Harada, K., and Tsunogai, S. (1996). Seasonal variations of residence time and upper atmospheric contribution of aerosols studied with Pb-210, Bi-210, Po-210 and Be-7. *Tellus B* 48, 690–702. doi: 10.3402/tellusb.v48i5.15940

Tsunogai, S., Uematsu, M., Noriki, S., Tanaka, N., and Yamada, M. (1982). Sediment trap experiment in the northern North Pacific: undulation of settling particles. *Geochem. J.* 16, 129–147. doi: 10.2343/geochemj.16.129

Tsunogai, S., Watanabe, Y. W., Harada, K., Watanabe, S., Saito, S., and Nakajima, M. (1993). *Dynamics of the Japan Sea Deep Water Studied With Chemical and Radiochemical Tracers, Elsevier Oceanography Series*. Amsterdam: Elsevier, 105–119. doi: 10.1016/S0422-9894(08)71321-7

Turekian, K. K. (1989). Lead-210 in the SEAREX program: an aerosol tracer across the Pacific. *Chem. Oceanogr.* 10, 51–81.

Turekian, K. K., Benninger, L. K., and Dion, E. P. (1983). ^{7}Be and ^{210}Pb total deposition fluxes at New Haven, Connecticut and at Bermuda. *J. Geophys. Res. Oceans* 88, 5411–5415. doi: 10.1029/JC088iC09p05411

Turekian, K. K., Nozaki, Y., and Benninger, L. K. (1977). Geochemistry of atmospheric radon and radon products. *Annu. Rev. Earth Planet. Sci.* 5, 227–255. doi: 10.1146/annurev.ea.05.050177.001303

Watanabe, Y., Watanabe, S., and Tsunogai, S. (1991). Tritium in the Japan Sea and the renewal time of the Japan Sea deep water. *Mar. Chem.* 34, 97–108. doi: 10.1016/0304-4203(91)90016-P

Yan, G., and Kim, G. (2015). Sources and fluxes of organic nitrogen in precipitation over the southern East Sea/Sea of Japan. *Atmos. Chem. Phys.* 15, 2761–2774. doi: 10.5194/acp-15-2761-2015

Yi, Y., Zhou, P., and Liu, G. (2007). Atmospheric deposition fluxes of ^{7}Be, ^{210}Pb and ^{210}Po at Xiamen, China. *J. Radioanal. Nucl. Chem.* 273, 157–162.

Zhang, F., Wang, J., Baskaran, M., Zhong, Q., Wang, Y., Paatero, J., et al. (2021). A global dataset of atmospheric ^{7}Be and ^{210}Pb measurements: annual air concentration and depositional flux. *Earth Syst. Sci. Data* 13, 2963–2994. doi: 10.5194/essd-13-2963-2021

Zheng, L., Minami, T., Konagaya, W., Chan, C.-Y., Tsujisaka, M., Takano, S., et al. (2019). Distinct basin-scale-distributions of aluminum, manganese, cobalt, and lead in the North Pacific Ocean. *Geochim. Cosmochim. Acta* 254, 102–121. doi: 10.1016/j.gca.2019.03.038

Zurbrick, C. M., Boyle, E. A., Kayser, R. J., Reuer, M. K., Wu, J., Planquette, H., et al. (2018). Dissolved Pb and Pb isotopes in the North Atlantic from the GEOVIDE transect (GEOTRACES GA-01) and their decadal evolution. *Biogeosciences* 15, 4995–5014. doi: 10.5194/bg-15-4995-2018

Zurbrick, C. M., Gallon, C. L., and Flegal, A. R. (2017). Historic and industrial lead within the Northwest Pacific Ocean evidenced by lead isotopes in seawater. *Environ. Sci. Technol.* 51, 1203–1212. doi: 10.1021/acs.est.6b04666

Conflict of Interest: The authors declare that the research was conducted in the absence of any commercial or financial relationships that could be construed as a potential conflict of interest.

Publisher's Note: All claims expressed in this article are solely those of the authors and do not necessarily represent those of their affiliated organizations, or those of the publisher, the editors and the reviewers. Any product that may be evaluated in this article, or claim that may be made by its manufacturer, is not guaranteed or endorsed by the publisher.